

Molecular Beam Epitaxial Growth and Device Characterization of AlGa_N Nanowire Ultraviolet-B Light-Emitting Diodes

M. Rajan Philip¹, T. H. Q. Bui¹, D. D. Choudhary¹, M. Djavid¹, P. Vu, T. T. Pham², H.-D. Nguyen³, H. P. T. Nguyen^{2,4*}

Abstract: We report on the design and fabrication of high performance Al_xGa_{1-x}N nanowire ultraviolet (UV) light-emitting diodes (LEDs) on silicon substrate by molecular beam epitaxy. The emission wavelength and surface morphology of nanowires can be controlled by varying the growth parameters that include substrate temperatures and/or Aluminum/Gallium flux ratios. The devices exhibit excellent current-voltage characteristics with relatively low resistance. Such nanowire LEDs generate strong emission in the UV-B band tuning from 290 nm to 330 nm. The electroluminescence spectra show virtually invariant blue-shift under injection current from 50 mA to 400 mA, suggesting the presence of a negligible quantum-confined Stark effect. Moreover, we have shown that, the AlGa_N nanowire LEDs using periodic structures, can achieve high light extraction efficiency of ~ 89% and 92% for emissions at 290nm and 320nm, respectively. The randomly arranged nanowire 290 nm UV LEDs exhibit light extraction efficiency of ~ 56% which is higher compared to current AlGa_N based thin-film UV LEDs.

Keywords: UV-B, nanowire LEDs, III-nitride, molecular beam epitaxy.

1. Introduction

A compact, highly efficient, and high-power UV light-source with emission wavelengths below 350 nm has attracted great attention due to its wide range of applications. The primary applications of such UV emitters include remote detection of biological and chemical compound, cancer detection and fluorescence sensing or Raman^[1]. The possibility of generating light sources using GaN based LEDs for photonic applications, with emission ranging from deep UV to near infrared by tuning the material bandgap makes them the versatile materials in the photonic industries^[2-4]. Optoelectronic devices working in the deep UV spectral region are being sought out because of their potential applications in disinfection^[5, 6], water purification^[7, 8], medical/biomedical instruments, and high-density optical LASER for recording^[9]. In contrast to the existing bulky and hazardous mercury UV lamp sources, UV LEDs offer high efficiency^[10, 11] and specific features like wavelength selectivity, compactness^[12, 13] and environmental-friendly light sources which make them a better choice to replace the future era devices. UV-B (290 - 320 nm) range of wavelength has been sought out for its capability of generating vitamin D in our body through exposure^[14, 15]. Moreover, UV-B emission is widely used for phototherapy which involves treatment of the skin, by exposing it to a UV-B source of light^[16, 17]. The latter procedure is

¹Department of Electrical and Computer Engineering, New Jersey Institute of Technology, 323 Martin Luther King Boulevard, Newark, New Jersey, 07102, United States.

²Faculty of Applied Sciences, Ho Chi Minh University of Technology, Vietnam National University in Ho Chi Minh City, 268 Ly Thuong Kiet, Ward 14, District 10, Ho Chi Minh City, 70001, Vietnam.

³Vietnam Academy of Science and Technology, Institute of Applied Materials Science, 1 Mac Dinh Chi Street, District 1, Ho Chi Minh City, 70001, Vietnam.

⁴Electronic Imaging Center, New Jersey Institute of Technology, 323 Martin Luther King Boulevard, Newark, New Jersey, 07102, United States.

*Corresponding Author: Hieu P. T. Nguyen. hieu.p.nguyen@njit.edu; Phone: +1-973-596-3523.

extremely useful to treat various diseases ranging from skin cancer, psoriasis, stimulating wound healing, stimulating the immune system and DNA analysis^[14, 15]. This particular spectrum has also found its use almost exclusively in the skin tanning industry. The UV-B lights, when incident to the skin, activates a pigment called melanin in epidermal skin, which aids or accelerates the process of tanning^[18]. Devices used traditionally for producing UV spectra of light are large and bulky, like UV lamps consisting of mercury. These devices exhibit low efficiency and lack of flexibility as well. The alternative approach for UV sources using highly efficient AlGaIn nanowire heterojunction structures seems to be far superior^[19-21].

To improve the performance of LEDs, their external quantum efficiency (EQE), which is directly proportional to the product of internal quantum efficiency (IQE) and light extraction efficiency (LEE), must be enhanced. Approaches that include patterned substrates^[22], rolled up nanotubes^[23], surface roughing^[24] and photonic crystal patterns^[25] have been used in the past to enhance the LEE of UV LEDs. In this regard, the III-nitrides targeted to reach the latter goal of UV LEDs has been limited by performance constraints on account of their extremely inefficient *p*-type doping^[26, 27] due to only small fraction of Mg being activated at room temperatures, large dislocation density^[28], which lead to low efficient, low output power LEDs. On account of this, III-nitride nanowire based UV LEDs exhibit exceptional performance compared to AlGaIn based thin-film UV LED structures resulted from the significantly improved light output power due to drastically reduced dislocations and polarization fields, and better effectiveness in *p*-type doping. Such great advantages pave the way for a candidate in boosting the IQE of UV LEDs^[29, 30]. In this context, we have fabricated high performance LEDs with emission wavelength can be tunable from 290 nm to 330 nm grown by molecular beam epitaxy (MBE). The devices exhibit relatively low resistance with excellent current-voltage characteristics. The electroluminescence (EL) spectra show negligible blue-shift under injection current from 50mA to 400mA, proving that the nanowire UV LEDs exhibit strong and stable emission with significantly reduced polarization fields and negligible quantum-confined Stark effect^[31, 32]. Moreover, using periodic nanowire structures, we have shown that, the UV LEDs can achieve high LEE of ~ 89% and 92% for emissions at 290nm and 320nm, respectively. The randomly arranged nanowire UV LEDs exhibit high LEE of ~ 56% which is higher compared to current AlGaIn based thin-film UV LEDs at similar wavelength emission.

2. Structural optimization and Simulation

Three-dimensional Finite-Difference Time Domain (FDTD) simulation is employed to analyze and calculate the LEE of the UV LEDs. The nanowire LED heterostructures are designed with emission wavelength in the UV-B band. The nanowire UV LED structure is schematically shown in Figure 1. The array is abab (hexagonal) form. Each nanowire consists of 250 nm *n*-GaIn, 100 nm *n*-AlGaIn, 60 nm quantum well (QW), 100 nm *p*-AlGaIn and 10 nm *p*-GaIn. The underlying substrate is Si (111). The device spans $2.5 \mu\text{m} \times 2.5 \mu\text{m}$, enclosed in 12 perfectly matched layers (PML) to absorb outgoing waves without causing any unwanted reflection of boundaries^[33, 34]. The parameters of PML (attenuation factor (σ)) and (auxiliary attenuation coefficient (κ)) are set to 0.25 and 2, respectively. Via Lumerical adaptive meshing^[35], the minimum mesh step size was set to 0.25 nm. The source to replicate the excitation was a single dipole source with Gaussian shape spectrum, and TM mode (electric field parallel to nanowire axial direction) is placed in the nanowire in the middle of the nanowire array, in the middle of the active region. In AlGaIn LEDs, the electric field direction parallel to the *c* axis which accounts for TE polarization which is the prominent emission in UV-B LEDs^[36, 37] is taken into perspective. The simulation wavelengths are chosen to be 290 nm and 320 nm to cover the UV-B. The ratio of the power emitted from the side surfaces of the LED

to the total emitted power of the device active region is considered as the LEE.

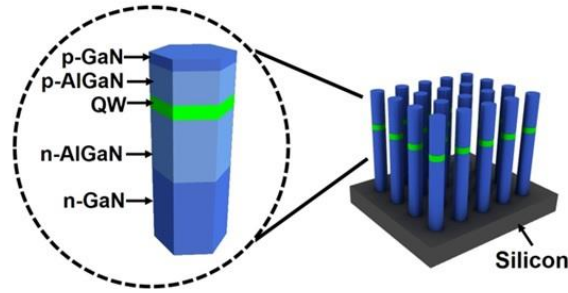


Figure 1: Schematic illustration of GaN based nanowire UV-B LED structure with inset image presenting the detailed structure of *n*-AlGaIn layer, a quantum well active region, a *p*-AlGaIn layer, and *p*-GaN layers.

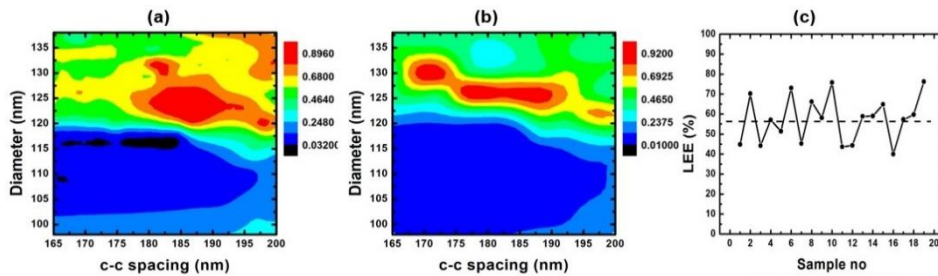


Figure 2: The contour plots for AlGaIn based nanowire UV-B emitters depicting LEEs with the radius ranges of 49–69 nm, and center to center (c-c) spacing ranges of 165–200 nm with light sources of (a) 290 nm (b) 320 nm and (c) LEE for 19 different random structures with different nanowire diameter and nanowire spacing between them for a light source of 290 nm.

To understand the dependency of LEE on the nanowire parameters including radius and spacing, a contour plot relating these three parameters can be seen in Figures 2(a) and 2(b). A relatively high LEE (92%) is acquired at a center to center spacing of ~170 nm and radius of 65 nm for emission at wavelength equal to 320 nm. Similarly, LEE of ~89% was calculated for nanowire UV LEDs with emission at 290 nm when the radius and spacing value are ~62 nm and 186 nm, respectively. The enhanced LEE values especially from lateral sides of the nanowire structure arises due to the mode coupling within the nanowires. During the generation of coupled modes, light propagates horizontally through the nanowires and thus can be extracted.

To replicate identical scenario to the fabricated nanowire structures via MBE spontaneous growth in which the nanowire diameter is varied in a range of 5%, we introduced a randomness of around 5% thus generating non-periodic structures with different nanowire radius and spacing and computed the LEE, as plotted in Figure 2 (c). The LEE of the random UV-B LED structure with a tolerance of 10% from the optimized conditions for LEE has an average LEE of ~56 %. This LEE value is lower than the periodic structures, however, it is still a high value in comparison to the existing UV-B LEDs at the same emission wavelength. This variation in LEE can be explained by the LED device switching within and outside the photonic band gap modes. The nanowire LED periodic arrays can be considered as active photonic crystal structures. However, photonic crystals themselves are utilized in photonic bandgap regions whereas the nanowire LED periodic array is utilized in the non-bandgap regions. Photonic bandgap regions are sets of wavelengths prohibited from propagating throughout the structure. Since the nanowire LED arrays prefer non-bandgap

regions, light propagates through the structure into surrounding air. Depending on the need of application, the nanowire photonic crystal structures have different operating regimes, namely, light confinement regime, which is used for lasers, and light transmission regime, used in LEDs^[36]. Nanowires with varying diameter and spacing result in the formation of different wave vectors, and hence different degrees of transmission at corresponding wavelengths. The low side LEE (blue area) represents the photonic bandgap region of periodic nanowire arrays or the inhibition of light propagation through the structure. The FDTD simulation utilized to acquire information about LEE of different nanowire array diameter and spacing using Particle Swarm Optimization (PSO). Therefore, careful control over spacing and radius is to be exercised to endure least possible total internal reflection at the semiconductor-air interface, which would aid the light to escape the device leading to a higher LEE and reduced material absorption in the deep UV LEDs^[38]. The effect of variation in spacing and radius can be seen by examining the contour plot. The LEE varies from 1% to 90%. The reason for this can be accounted to the formation of coupled modes, leading to a jump in LEE.

3. Experimental details

The AlGaIn nanowire UV-B LED heterostructure, illustrated in Figure 1, was spontaneously formed on Si (111) substrates under nitrogen rich conditions by a Veeco Gen-II MBE system equipped with a radio-frequency plasma-assisted nitrogen source. The nanowire diameter and density can be controlled by controlling the substrate temperature and/or Al/Ga flux ratios, while the nanowire length was varied mostly by the growth duration. The nanowire size was selected according to the results obtained from the simulation/design task. Figure 1 depicts the schematic structure of GaN/AlGaIn UV-B nanowire LED structure on Si substrate. The inset of Figure 1 presents the detailed structure of LED. The device fabrication route of AlGaIn nanowire UV LEDs involves the following steps. Initially, for planarization and passivation, the nanowire arrays were spin-coated with polyimide resist solution, illustrated in Figure 3(a). This was followed by O₂ dry etching to expose the top region of the nanowires, shown in Figure 3(b). Metal contact layer including Ni (5 nm)/Au (5 nm)/indium tin oxide (ITO) was then deposited to the exposed GaN:Mg surface to form top metal contacts. Shown in Figure 3(c), Ti/Au (10 nm/100 nm) and metal-grid Ni/Au (10 nm/100 nm) layers were then evaporated on the backside of the Si substrate and top of ITO to form the backside and topside contacts, respectively. Additional information regarding the MBE growth and device fabrication of such nanowire LEDs can be found elsewhere^[2, 4].

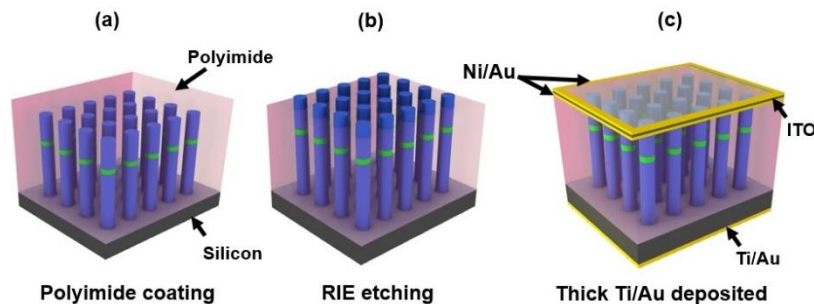


Figure 3: Fabrication procedure of UV-B nanowire LEDs on Si substrate.

Surface morphology of the UV nanowire LED heterostructures was studied by scanning electron microscopy (SEM). The nanowire UV-B LEDs exhibit quite uniform surface morphology and high density, as illustrated in Figure 4.

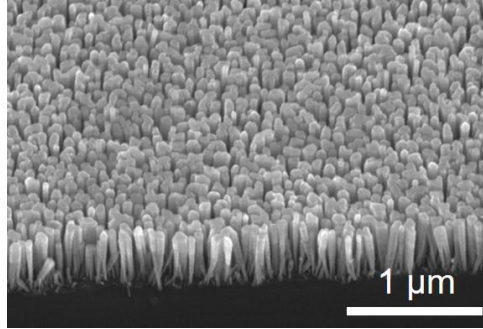


Figure 4: 45° cross-sectional SEM image of nanowires grown on silicon wafer.

4. Results and discussion

Optical properties of AlGaIn nanowire UV LEDs were examined using a 266 nm diode-pumped solid-state (DPSS) Q-switched laser as the excitation source. The duration, maximum energy, and repetition rate of the laser pulse are 7ns, 4uJ and 7.5 kHz, respectively. To eliminate the emission from the excitation laser source, a long pass filter (> 270nm) was placed in front of the spectrometer.

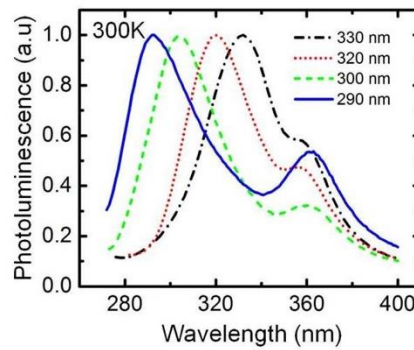


Figure 5: Normalized room temperature photoluminescence spectra of UV-B lights at 290 nm, 300 nm, 320 nm and 330 nm from multiple AlGaIn nanowire LEDs.

Figure 5 presents the room temperature PL spectra of nanowire LEDs with the peak wavelengths were measured at 290 nm, 300 nm, 320 nm, 330 nm respectively. As seen from the corresponding plots, the peaks match the designed wavelength of the light excited from the nanowire LEDs. Alteration of Al composition in the AlGaIn quantum dots can be achieved either by using different growth temperatures and/or Al/Ga flux ratios. In the room temperature PL spectra, Al composition increases for a lower wavelength (or higher bandgap material) emission in the electromagnetic spectrum. Thus, for tuning the emission from 290 nm to 330 nm UV-B regime, Al composition is increased in the active regions. The emission peak at ~ 365 nm is corresponded to the emission from GaN segment.

Figure 6 shows the EL spectra of the AlGaIn nanowire UV-B LED with emission wavelength at 320 nm. The EL spectra were measured at room temperature using the Ocean Optics spectrometer (USB 2000) at injection currents from 50 mA to 400 mA for device area of 500μm × 500μm. The devices were measured under pulsed biasing conditions (~1% duty cycle) to minimize junction heating effect.

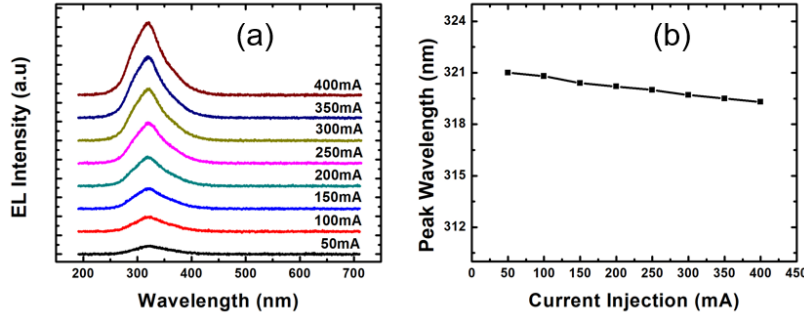


Figure 6: (a) Electroluminescence spectra of GaN/AlGaN based UV-B nanowire LED from 50 mA to 450 mA (b) variation of peak wavelength with current injection.

The EL spectra exhibits a singular peak at around 320 nm which corresponds to the emission from the AlGaN quantum well, shown in Figure 6(a). Additionally, illustrated in Figure 6(b), the emission peak position shows very small shifts (1.5 nm) with increasing injection current, emphasizing the presence of a negligible polarization field due to the effective strain relaxation. It can be observed that the device shows a stable and strong emission at 320 nm independent of injection currents even with the absence of emission on the visible wavelength range; which was observed in AlGaN QW based UV LEDs, due to the deep level defects in AlGaN^[39, 40]. This clean EL spectrum is crucial in the improvement of the signal-noise ratio.

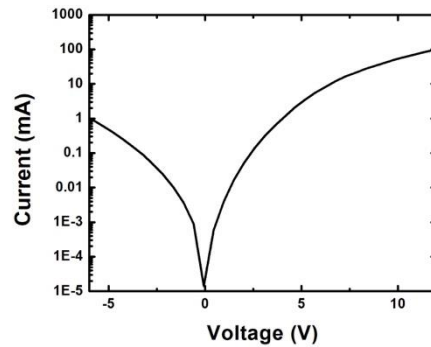


Figure 7: Current–voltage characteristics of the AlGaN nanowire LED.

Current-voltage characteristics of the UV LEDs are depicted in Figure 7. The defect density, internal electric field induced quantum confined Stark effect and polarization field, are minimized in nanowires in contrast to thin films, resulting in perfect diode performances with very low leakage current which is <1mA at reverse voltage of ~ -6V. The sharp increase of current in the forward bias confirms excellent current-voltage characteristics with low resistance. The leakage current can be attributed to the leakage paths arising due to the inadequate insulation between the nanowires and the polyimide resist as well as due to carrier recombination happening in active region of LED near the nanowire sidewalls due to surface states present^[41].

5. Conclusions

In summary, we have demonstrated high performance UV-B LEDs using novel AlGaN nanowire LEDs with high crystal quality on a large silicon substrate. The LEE of such nanowire UV-B LEDs has been significantly improved. The UV LEDs hold strong EL intensity with negligible blue shift. This study addresses some of the major issues with reference to the practical applications of

nanowire LEDs and provides a novel perspective of having high efficiency UV-B LEDs with tunable emission for medical applications.

Acknowledgement: This work was supported by New Jersey Institute of Technology.

References:

1. **N. Narendran, Y. Gu**, "Life of LED-Based White Light Sources," *J. Display Technol.* **1**(1), 167-171 (2005).
2. **M. R. Philip, D. D. Choudhary, M. Djavid, M. N. Bhuyian, et al.**, "Controlling color emission of InGaN/AlGaIn nanowire light-emitting diodes grown by molecular beam epitaxy," *J Vac Sci Technol B Nanotechnol Microelectron.* **35**(2), 02B108 (2017).
3. **M. R. Philip, D. D. Choudhary, M. Djavid, K. Q. Le, et al.**, "High efficiency green/yellow and red InGaN/AlGaIn nanowire light-emitting diodes grown by molecular beam epitaxy," *JSAMD.* **2**(2), 150-155 (2017).
4. **M. Rajan Philip, D. D. Choudhary, M. Djavid, M. N. Bhuyian, et al.**, "Fabrication of Phosphor-Free III-Nitride Nanowire Light-Emitting Diodes on Metal Substrates for Flexible Photonics," *ACS Omega.* **2**(9), 5708-5714 (2017).
5. **J. Close, J. Ip, K. H. Lam**, "Water recycling with PV-powered UV-LED disinfection," *Renewable Energy.* **31**(11), 1657-1664 (2006).
6. **M. A. Würtele, T. Kolbe, M. Lipsz, A. Külberg, et al.**, "Application of GaN-based ultraviolet-C light emitting diodes – UV LEDs – for water disinfection," *Water Res.* **45**(3), 1481-1489 (2011).
7. **M. Mori, A. Hamamoto, A. Takahashi, M. Nakano, et al.**, "Development of a new water sterilization device with a 365 nm UV-LED," *MBEC.* **45**(12), 1237-1241 (2007).
8. **A. Hamamoto, M. Mori, A. Takahashi, M. Nakano, et al.**, "New water disinfection system using UVA light-emitting diodes. *Appl. Microbiol.*" **103**(6), 2291-2298 (2007).
9. **D. Xu**, *Multi-dimensional Optical Storage*, 1st ed. edition, Springer (2016).
10. **H. Hideki, A. Katsushi, K. Takashi, N. Takao, et al.**, "High-Efficiency 352 nm Quaternary InAlGaIn-Based Ultraviolet Light-Emitting Diodes Grown on GaN Substrates," *Jpn. J. Appl. Phys.* **43**(10A), L1241-L1243 (2004).
11. **K. Nagamatsu, N. Okada, H. Sugimura, H. Tsuzuki, F. Mori, et al.**, "High-efficiency AlGaIn-based UV light-emitting diode on laterally overgrown AlN," *J. Cryst. Growth.* **310**(7), 2326-2329 (2008).
12. **K. Davitt, Y.-K. Song, W. R. Patterson, A. V. Nurmikko, et al.**, "Spectroscopic Sorting of Aerosols by a Compact Sensor Employing UV LEDs," *Aerosol Sci. Technol.* **40**(12), 1047-1051 (2006).
13. **S. Ek, B. Anderson, S. Svanberg**, "Compact fiber-optic fluorosensor employing light-emitting ultraviolet diodes as excitation sources," *Spectrochimica Acta Part B: At. Spectrosc.* **63**(2), 349-353 (2008).
14. **T. A. Kalajian, A. Aldoukhi, A. J. Veronikis, K. Persons, et al.**, "Ultraviolet B Light Emitting Diodes (LEDs) Are More Efficient and Effective in Producing Vitamin D3 in Human Skin Compared to Natural Sunlight," *Sci. Rep.* **7**(1), 11489 (2017).
15. **P. Chandra, L. L. Wolfenden, T. R. Ziegler, J. Tian, et al.**, "Treatment of vitamin D deficiency with UV light in patients with malabsorption syndromes: a case series," *Photodermatol Photoimmunol Photomed.* **23**(5), 179-185 (2007).
16. **A. Reich, K. Mędrek**, "Effects of Narrow Band UVB (311 nm) Irradiation on Epidermal Cells," *Int. J. Mol. Sci.* **14**(4), 8456-8466 (2013).

17. **G. D. Bandow, J. Y. M. Koo**, “Narrow-band ultraviolet B radiation: a review of the current literature,” *Int. J. dermatol.* **43**(8), 555-561 (2004).
18. **A. Kawada**, “UVB-induced erythema, delayed tanning, and UVA-induced immediate tanning in Japanese skin,” *Photodermatol.* **3**(6), 327-333 (1986).
19. **S. Krishnamoorthy, F. Akyol, P. S. Park, S. Rajan**, “Low resistance GaN/InGaN/GaN tunnel junctions,” *Appl. Phys. Lett.* **102**(11), 113503 (2013).
20. **A. Yasan, R. McClintock, S. R. Darvish, Z. Lin, et al.**, “Characteristics of high-quality p-type Al_xGa_{1-x}N/GaN superlattices,” *Appl. Phys. Lett.* **80**(12), 2108-2110 (2002).
21. **J. Simon, V. Protasenko, C. Lian, H. Xing, et al.**, “Polarization-Induced Hole Doping in Wide-Band-Gap Uniaxial Semiconductor Heterostructures,” *Sci.* **327**(5961), 60-64 (2010).
22. **Y. Motokazu, M. Tomotsugu, N. Yukio, S. Shuji, et al.**, “InGaN-Based Near-Ultraviolet and Blue-Light-Emitting Diodes with High External Quantum Efficiency Using a Patterned Sapphire Substrate and a Mesh Electrode,” *Jpn. J. Appl. Phys.* **41**(12B), L1431-L1433 (2002).
23. **M. Djavid, X. Liu, Z. Mi**, “Improvement of the light extraction efficiency of GaN-based LEDs using rolled-up nanotube arrays,” *Opt. Express.* **22**(S7), A1680-A1686 (2014).
24. **C. E. Lee, B. S. Cheng, Y. C. Lee, H. C. Kuo, et al.**, “Output Power Enhancement of Vertical-Injection Ultraviolet Light-Emitting Diodes by GaN-Free and Surface Roughness Structures. *Electrochem. solid state Lett.* **12**(2), H44-H46 (2009).
25. **J. Shakya, K. H. Kim, J. Y. Lin, H. X. Jiang**, Enhanced light extraction in III-nitride ultraviolet photonic crystal light-emitting diodes,” *Appl. Phys. Lett.* **85**(1), 142-144 (2004).
26. **N. Shuji, S. Masayuki, I. Naruhito, N. Shin-ichi, et al.**, “Superbright Green InGaN Single-Quantum-Well-Structure Light-Emitting Diodes,” *Jpn. J. Appl. Phys.* **34**(10B), L1332-L1335 (1995).
27. **S. Fischer, C. Wetzel, E. E. Haller, B. K. Meyer**, “On p-type doping in GaN—acceptor binding energies,” *Appl. Phys. Lett.* **67**(9), 1298-1300 (1995).
28. **John E. Ayers, T. Kujofsa, Paul Rago, Johanna Raphael**, *Heteroepitaxy of Semiconductors: Theory, Growth, and Characterization.* CRC Press (2016)..
29. **S. Zhao, A. T. Connie, M. H. T. Dastjerdi, X. H. Kong, et al.**, “Aluminum nitride nanowire light emitting diodes: Breaking the fundamental bottleneck of deep ultraviolet light sources,” *Sci. Rep.* **5**, 8332 (2015).
30. **X. Tang, G. Li, S. Zhou**, “Ultraviolet Electroluminescence of Light-Emitting Diodes Based on Single n-ZnO/p-AlGaIn Heterojunction Nanowires,” *Nano Lett.* **13**(11), 5046-5050 (2013).
31. **W. Guo, M. Zhang, A. Banerjee, P. Bhattacharya**, “Catalyst-Free InGaN/GaN Nanowire Light Emitting Diodes Grown on (001) Silicon by Molecular Beam Epitaxy,” *Nano Lett.* **10**(9), 3355-3359 (2010).
32. **Hon-Way Lin, Y.-J. LU, Hung-Ying Chen, Hong-Mao Lee, et al.**, “InGaN/GaN nanorod array white light-emitting diode,” *Appl. Phys. Lett.* **97**, 073101 (2010).
33. **J. P. Berenger**, “Perfectly matched layer for the FDTD solution of wave-structure interaction problems,” *IEEE Trans. Antennas Propag.* **44**(1), 110-117 (1996).
34. **J. P. Berenger**, “Evanescent waves in PML's: origin of the numerical reflection in wave-structure interaction problems,” *IEEE Trans. Antennas Propag.* **47**(10), 1497-1503 (1999).
35. **L. Yaxun, C. D. Sarris**, “AMR-FDTD: a dynamically adaptive mesh refinement scheme for the finite-difference time-domain technique,” *Proc. IEEE Antennas and Propagat. Soc. Int. Symp.* **1A**, 134–137 (2005)..

36. **M. Djavid, Z. Mi**, “Enhancing the light extraction efficiency of AlGa_N deep ultraviolet light emitting diodes by using nanowire structures,” *Appl. Phys. Lett.* **108**(5), 051102 (2016).
37. **T. Kolbe, A. Knauer, C. Chua, Z. Yang, et al.**, “Optical polarization characteristics of ultraviolet (In)(Al)Ga_N multiple quantum well light emitting diodes,” *Appl. Phys. Lett.* **97**(17), 171105 (2010).
38. **M. Djavid, D. Choudhary, M. Rajan Philip, T. H. Q. Bui, et al.**, “Effects of Optical Absorption in Deep Ultraviolet Nanowire Light-Emitting Diodes,” *Phot. Nano. Fund. Appl* (In press) DOI: 10.1016/j.photonics.2017.10.003 (2017).
39. **J. Zhang, S. Wu, S. Rai, V. Mandavilli, et al.**, “AlGa_N multiple-quantum-well-based, deep ultraviolet light-emitting diodes with significantly reduced long-wave emission,” *Appl. Phys. Lett.* **83**(17), 3456-3458 (2003).
40. **K. X. Chen, Y. A. Xi, F. W. Mont, J. K. Kim, et al.**, “Recombination dynamics in ultraviolet light-emitting diodes with Si-doped Al_xGa_{1-x}N/Al_yGa_{1-y}N multiple quantum well active regions,” *J. Appl. Phys.* **101**(11), 113102 (2007).
41. **J. Bai, Q. Wang, T. Wang**, “Characterization of InGa_N-based nanorod light emitting diodes with different indium compositions,” *J. Appl Phys.* **111**(11), 113103 (2012).